Nanoscale Res Lett (2009) 4:1078–1084
DOI 10.1007/s11671-009-9356-0

NANO EXPRESS

Preparation and Characterization of Silica-Coated Magnetic–Fluorescent Bifunctional Microspheres

Qi Xiao · Chong Xiao

Received: 11 December 2008 / Accepted: 24 May 2009 / Published online: 20 June 2009

Abstract Bifunctional magnetic–fluorescent composite nanoparticles (MPQDs) with Fe_3O_4 MPs and Mn:ZnS/ZnS core–shell quantum dots (QDs) encapsulated in silica spheres were synthesized through reverse microemulsion method and characterized by X-ray powder diffraction, scanning electron microscopy, transmission electron microscopy, vibration sample magnetometer, and photoluminescence (PL) spectra. Our strategy could offer the following features: (1) the formation of Mn:ZnS/ZnS core/shell QDs resulted in enhancement of the PL intensity with respect to that of bare Mn:ZnS nanocrystals due to the effective elimination of the surface defects; (2) the magnetic nanoparticles were coated with silica, in order to reduce any detrimental effects on the QD PL by the magnetic cores; and (3) both Fe_3O_4 MPs and Mn:ZnS/ZnS core–shell QDs were encapsulated in silica spheres, and the obtained MPQDs became water soluble. The experimental conditions for the silica coating on the surface of Fe_3O_4 nanoparticles, such as the ratio of water to surfactant (R), the amount of ammonia, and the amount of tetraethoxysilane, on the photoluminescence properties of MPQDs were studied. It was found that the silica coating on the surface of Fe_3O_4 could effectively suppress the interaction between the Fe_3O_4 and the QDs under the most optimal parameters, and the emission intensity of MPQDs showed a maximum. The bifunctional MPQDs prepared under the most optimal parameters have a typical diameter of 35 nm and a saturation magnetization of 4.35 emu/g at room temperature and exhibit strong photoluminescence intensity.

Q. Xiao (✉) · C. Xiao
School of Resources Processing and Bioengineering, Central South University, 410083 Changsha, China
e-mail: xiaoqi88@mail.csu.edu.cn

Keywords Bifunctional microspheres · Magnetic · Fluorescent

Introduction

Semiconductor quantum dots (QDs) have been widely explored as biomedical labeling agents [1–4]. However, the small-ensemble Stokes shift of intrinsic QDs can cause self-quenching. In addition, experimental results indicated that any leakage of cadmium from the QDs would be toxic and fatal to biological system [5], and cadmium-containing products can be environmentally problematic. Recently, Peng et al. [6–8] reported that doped QDs could not only replace cadmium in CdSe QDs with zinc, but also overcome a number of intrinsic disadvantages of undoped QDs emitters, i.e., strong self-quenching caused by their small-ensemble Stokes shift (energy difference between absorption spectrum and emission band) [9] and sensitivity to thermal, chemical, and photochemical disturbances [10]. Mn^{2+}-doped ZnS QDs have been extensively investigated for use in various applications other than biomedical labeling, such as displays, sensors, and lasers [11–13]. In addition, the luminescence lifetime of Mn^{2+}-doped ZnS QDs is $\sim$1 ms. Such a long lifetime makes the luminescence from the nanocrystal readily distinguishable from any background luminescence. Therefore, Mn^{2+}-doped ZnS QDs could be potential candidates as fluorescent labeling agents, especially in biology [14]. Magnetic nanoparticles of iron oxides (MPs) also show many advantages in biological applications. One unique feature of magnetic nanoparticles is to respond well to magnetic control, which has led to several successful applications, including biological separation, protein purification, bacteria detection, and drug delivery [15, 16]. Highly

luminescent QDs could serve as luminescent markers, while magnetic nanoparticles could be easily manipulated under the external magnetic field. Therefore, combination of QDs and MPs to get fluorescent–magnetic bifunctional composite nanoparticles (MPQDs) has attracted intense attention in the past decade due to its appealing applications [17–25]. Surface modification of QDs and MPs with silica has led to improved stability, lower toxicity, and higher biocompatibility, and protection of the QDs against corrosion by the biological buffer. In addition, the rich and well-known surface chemistry of silica makes bioconjugation more convenient. However, it was still a challenge to obtain magnetic, multicolor barcoded nanospheres with controllable size and tunable readout.

In this work, we obtained water-soluble bifunctional MPQDs with Fe_3O_4 MPs and Mn:ZnS/ZnS core–shell QDs encapsulated in silica spheres through reverse microemulsion method. The synthetic procedure was illustrated in Scheme 1. Our strategy could offer the following features: (1) the formation of Mn:ZnS/ZnS core/shell QDs resulted in enhancement in the photoluminescence (PL) intensity with respect to that of bare Mn:ZnS nanocrystals due to the effective elimination of the surface defects, and the QDs' chemical stability and photostability were also preserved [26]; (2) the magnetic MPs were coated with silica, so that no interference of the QD PL by the magnetic particles was expected [20, 27]; and (3) both Fe_3O_4 MPs and Mn:ZnS/ZnS core–shell QDs were encapsulated in silica spheres, and the obtained MPQDs became water soluble. The obtained bifunctional MPQDs were characterized by X-ray powder diffraction (XRD), scanning electron microscopy (SEM), transmission electron microscopy (TEM), vibration sample magnetometer (VSM), and PL spectra. Besides the intensive PL, the MPQDs simultaneously exhibited magnetic properties and could be separated from solution using a permanent magnet. In a few words, the PL, magnetic, and water-soluble properties of the MPQDs would allow them to find a large range of applications for biolabeling, bioseparation, immunoassay, and diagnostics.

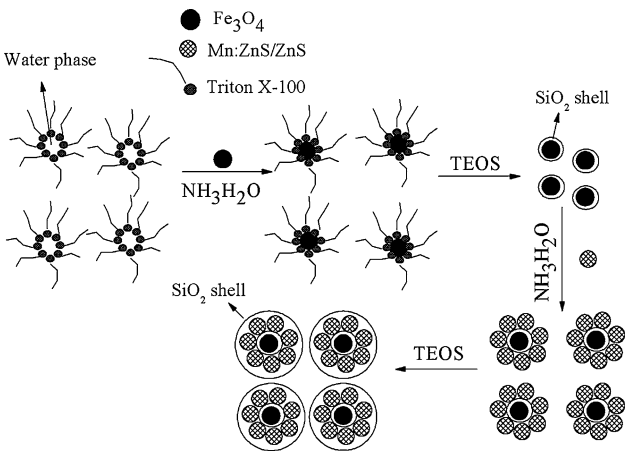

Scheme 1 Synthesis of bifunctional magnetic fluorescent composite nanoparticles

Experimental Section

Chemicals

All chemicals used were of analytical grade. Zn $(CH_3COO)_2{\cdot}2H_2O$, $Mn(CH_3COO)_2{\cdot}2H_2O$, $Na_2S{\cdot}9H_2O$, $FeCl_2{\cdot}4H_2O$, $FeCl_3{\cdot}6H_2O$, $Na_2SiO_3{\cdot}9H_2O$, and thioglycolic acid (TGA) were obtained from Shanghai Chemical Reagents Company, tetraethoxysilane (TEOS), ammonia (NH_4OH, 25–28 wt%), ethanol (95%), *n*-hexanol, cyclohexane, and acetone were obtained from Tianjin Hengxing Chemical Preparation Company; and TritonX-100 was obtained from Sinopharm Chemical Reagent Company. All chemicals were used as received. High-purity water with a resistivity of 18.2 MΩ/cm was used for preparation of all aqueous solutions.

Synthesis

Synthesis of Mn:ZnS/ZnS Core/Shell Quantum Dots

Mn:ZnS/ZnS core/shell QDs were synthesized according to our recent reports [26]. Briefly, the stock solution was prepared by adding $Zn(CH_3COO)_2{\cdot}2H_2O$ and $Mn(CH_3COO)_2{\cdot}2H_2O$ into 100 mL 0.12 M TGA aqueous solution respectively. The Mn/Zn molar ratios in the four samples were fixed at 1%. Then the TGA–manganese solution reacted with Na_2S aqueous solution at 80 °C for 20 min to form small-size MnS core. In order to obtain Mn:ZnS/ZnS core/shell QDs, the TGA–zinc complex aqueous solution was injected into the MnS core solution at two-step. At the first step, 75% of TGA–zinc solution was injected into the MnS core solution under vigorously stirring and heated at 80 °C for 10 h. The remaining TGA–zinc solution was then injected into the mixture and heated at 80 °C for another 2 h. The Mn:ZnS/ZnS core/shell QDs were obtained by adding excess ethanol to the solutions and then dried in vacuum.

Synthesis of Fe_3O_4 Nanoparticles

Fe_3O_4 nanoparticles were synthesized as reported by Massart et al. [28]. A mixture of 5.406 g of $FeCl_3{\cdot}6H_2O$ and 2.780 g of $FeCl_2{\cdot}4H_2O$ dissolved in 100 mL of high-purity water was placed in a 250-mL flask, following by the quick droplet-addition of 15 mL of 25% NH_4OH. The mixture was irradiated with high-intensity ultrasound (600 W, 20 kHz) at room temperature in ambient air for

1 h. After irradiation, the precipitate was centrifuged and washed using distilled water and ethanol for several times. It was then freeze-dried at 223 K for 4 h in vacuum.

Synthesis of Core–Shell Fe_3O_4@SiO_2 Nanoparticles

The core–shell Fe_3O_4@SiO_2 nanoparticles were synthesized as follows: 1 g of Fe_3O_4 nanoparticles were added to 100 mL of 2.84 wt% sodium silicate solution and ultrasonically dispersed for 30 min. Then, 2 wt% H_2SO_4 was used to adjust pH value of the solution to 9. The mixture was irradiated with high-intensity ultrasound (600 W, 20 kHz) at room temperature in ambient air for 1 h. Twenty-five milliliters cyclohexane, 3.2 mL *n*-hexanol, 8 mL TritonX-100, 1 mL of the as-prepared magnetic sol, and 1.5 mL of TEOS were added in a flask in turn under vigorous magnetic stirring. Thirty minutes after the microemulsion was formed, 1 mL NH_4OH (25 wt%) was added to initiate the polymerization process. The silica growth was completed after 10 h of stirring. The final product was denoted as FS.

Synthesis of Silica-coated Magnetic–luminescent Bifunctional Nanocomposites

One milliliter of Mn:ZnS/ZnS aqueous solution (10 g/L), 1 mL TEOS, and 1 mL NH_4OH (25 wt%) were in turn added into the above-mentioned FS and allowed to stir at room temperature for 5 h. Acetone was used to terminate the reaction, and the resultant precipitates of MPQDs were washed with water and ethanol for three times, and then dried in vacuum.

Characterization

The XRD patterns of the synthesized samples were obtained by a D/max-γA diffractometer using CuKα radiation ($\lambda = 0.15418$ nm). The size and morphology of the as-synthesized products were determined by a XL30 S-FEG SEM and a JEM-3010 high-resolution TEM. The PL spectra of the samples were recorded with a Fluorescence Spectrophotometer F-4500. The room temperature magnetization in the applied magnetic field was performed by model JDM-13 vibrating sample magnetometer.

Results and Discussions

Structural and Morphological Characterization

X-ray diffraction patterns of the samples are shown in Fig. 1. The indexing of the reflections demonstrated that the major components in MPQDs were cubic Fe_3O_4

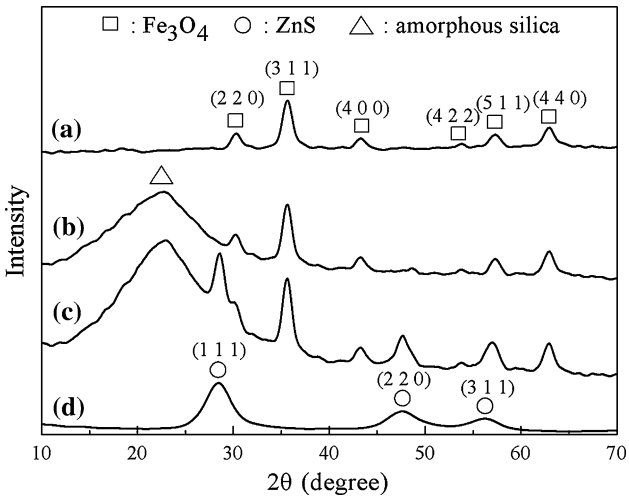

Fig. 1 XRD patterns of bare MPs (**a**), Fe_3O_4/SiO_2 (**b**), MPQDs (**c**), and Mn:ZnS/ZnS QDs (**d**)

(JCPDS no. 79-0418), zinc blende ZnS (JCPDS no. 77-2100), and amorphous SiO_2. The averaged crystallite size D was determined according to the Scherrer equation $D = K\lambda/\beta\cos\theta$ [29], where k was a constant (shape factor, about 0.9), λ was the X-ray wavelength (0.15418 nm), β was the full width at half maximum (FWHM) of the diffraction line, and θ was the diffraction angle. Based on the FWHM of (3 1 1) Fe_3O_4 and (111) zinc blende reflection, the averaged crystallite sizes of Fe_3O_4 and $Mn^{2\pm}$:ZnS/ZnS were estimated to be 14 and 5 nm respectively.

In order to obtain detailed information about the microstructure and morphology of the Fe_3O_4/SiO_2 and MPQDs sample, SEM and TEM observations were carried out, and the results of the Fe_3O_4/SiO_2 and MPQDs samples are shown in Figs. 2 and 3 respectively. A typical SEM image (Fig. 2a, b) shows that the Fe_3O_4/SiO_2 sample is composed of nanoparticles with a size in the range of about 20–40 nm. Figure 2c is the energy-dispersive X-ray (EDX) spectrum from Fig. 2b, further confirming that the Fe_3O_4/SiO_2 sample is composed of Fe, Si, and O, which is consistent with the XRD results (shown in Fig. 1b). A typical TEM image (Fig. 2d) shows that the size of Fe_3O_4/SiO_2 sample is about 15 nm. A typical SEM image (Fig. 3a, b) shows that the MPQDs sample is composed of nanoparticles with a size in the range of about 30–50 nm. Figure 3c is the EDX spectrum from Fig. 3b, further confirming that the MPQDs sample is composed of Fe, Si, O, Zn, and S, which is consistent with the XRD results (shown in Fig. 1c). A typical TEM image (Fig. 3d) shows that the size of the MPQDs sample is in the range of about 30 nm.

Optical Properties

Agekyan [30] reported that the interaction between the Fe_3O_4 and the QDs would influence the PL properties of

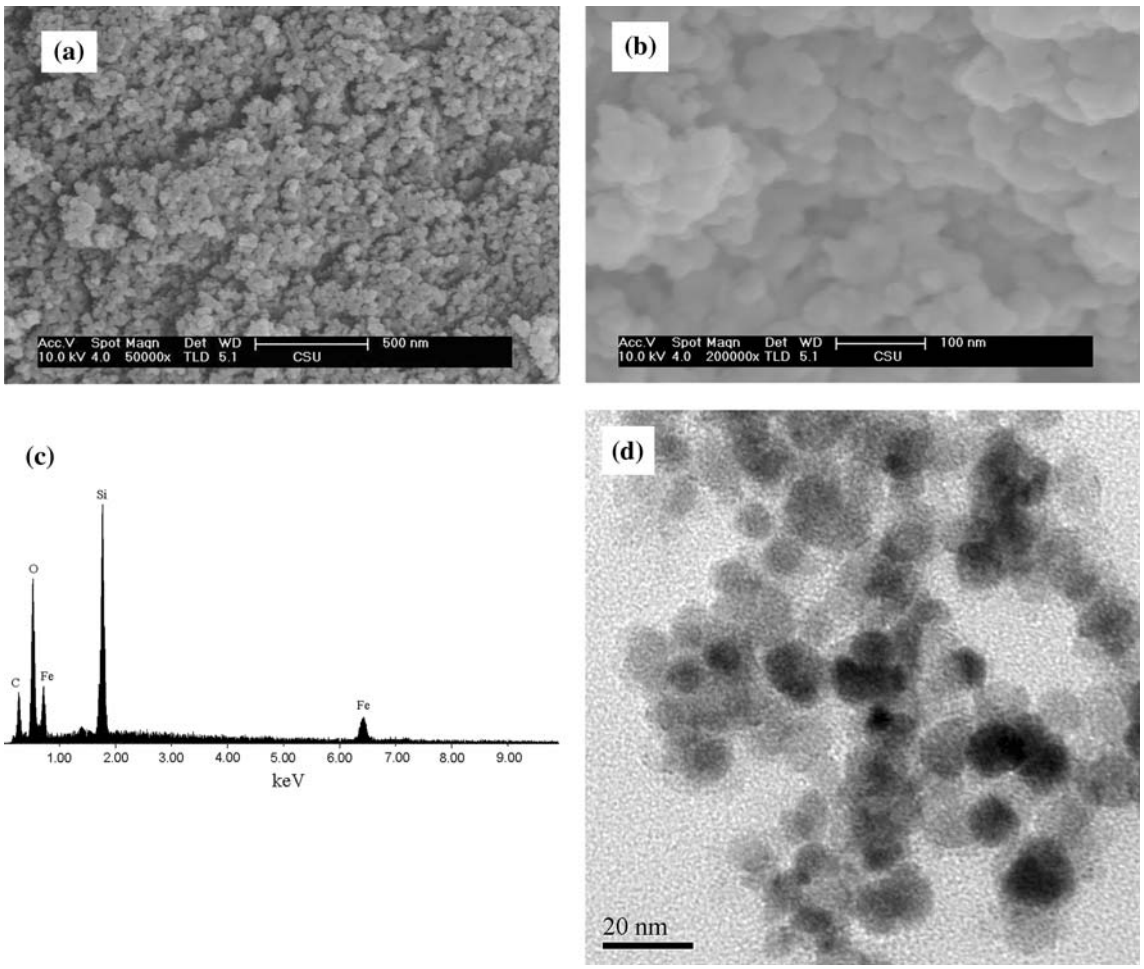

Fig. 2 **a**, **b** SEM image, **c** EDX spectrum from **a**, and **d** TEM image of the as-synthesized Fe_3O_4/SiO_2 nanoparticles

the nanocomposites. Hong et al. [31] reported that the PL properties of the magnetic–luminescent nanocomposites ($Fe_3O_4/PE_n/CdTe$) were very sensitive to the distance between Fe_3O_4 nanoparticles and CdTe QDs separated by the polyelectrolyte multilayers. The interaction between the two particle types was suppressed only after having deposited 21 layers of polyelectrolyte between the magnetic and the luminescent nanoparticles. In this paper, a dense silica shell was deposited on Fe_3O_4 nanoparticles in order to prevent quenching of the QDs by the magnetic Fe_3O_4 nanoparticles. Hence, control of silica coating on the surface of Fe_3O_4 nanoparticles is an important consideration. With this in mind, we investigated several experimental parameters for silica formation with the aim of optimizing the resulting MPQDs fluorescence.

The Effects of the Ratio of Water to Surfactant

Figure 4 showed the effect of the ratio of water to surfactant on the photoluminescence spectra of the MPQDs. It was found that the PL intensity increased with the decrease in the ratio of water to surfactant, and reached a maximum when R was 1:8. If the ratio of water to surfactant continued to decrease, namely <1:8, the PL intensity would decrease. Stjerndahl et al. [32] have reported that the SiO_2 shell thinned with the increasing water concentration. We have found that the optimal SiO_2 thickness was achieved when R was 1:8.

The Effect of the Amount of TEOS

Figure 5 showed the effect of the amount of TEOS on the photoluminescence spectra of the MPQDs. It was found that the PL intensity increased with the decrease in the amount of TEOS, and reached a maximum when TEOS was 1.5 mL. If the amount of TEOS was too low, a silica shell did not form on the surface of the Fe_3O_4 nanoparticles, while if the amount of TEOS was too high, loser and larger silica particles would form.

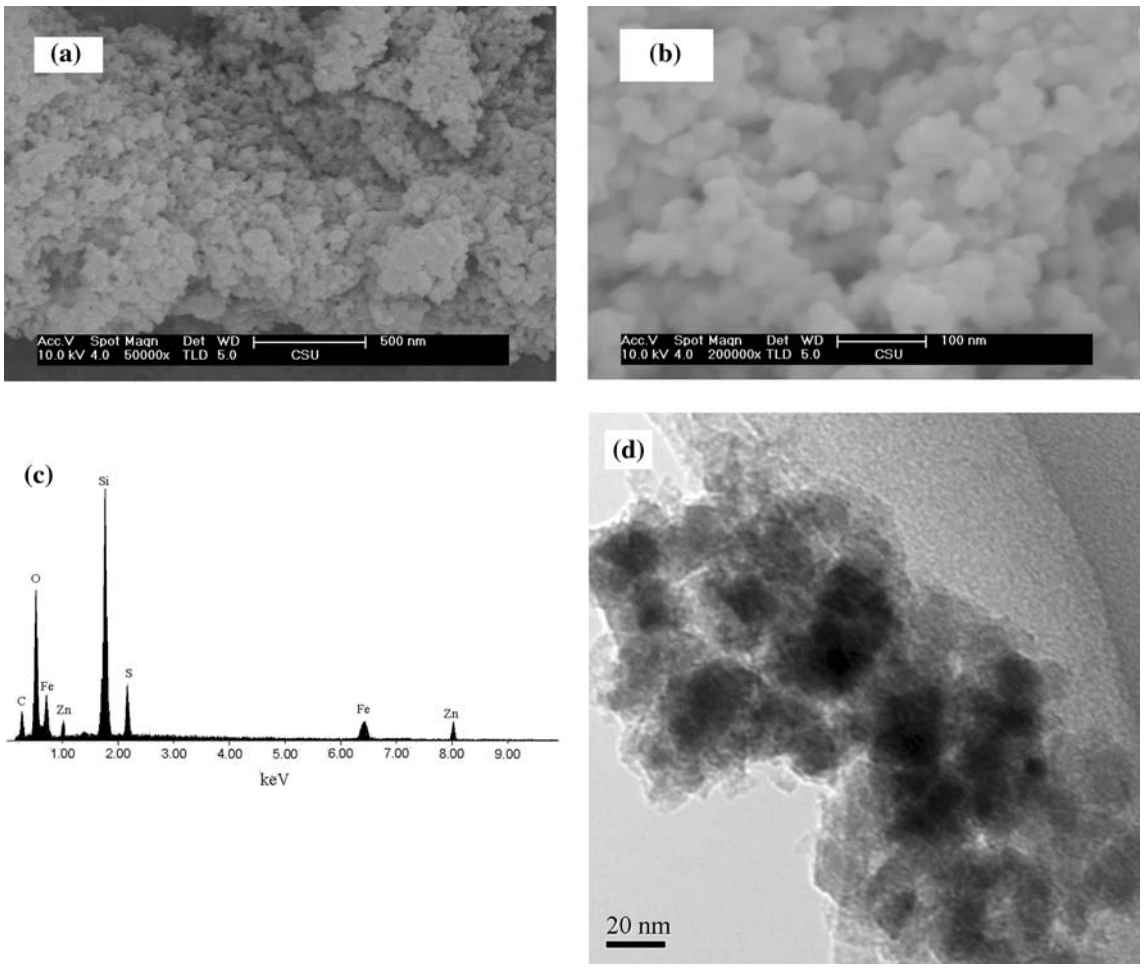

Fig. 3 **a**, **b** SEM image, **c** EDX spectrum from Fig. 2a, and **d** TEM image of the as-synthesized MPQDs

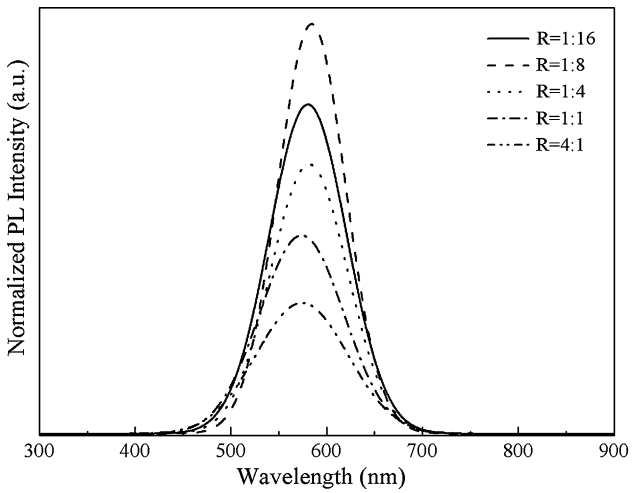

Fig. 4 The effects of the ratio of water to surfactant (R) on the photoluminescence spectra of the MPQDs

The Effect of the Amount of NH_4OH

Figure 6 showed the effect of the amount of NH_4OH on the photoluminescence spectra of the MPQDs. It was found that the PL intensity increased with the increase in the amount of NH_4OH, and reached a maximum when NH_4OH was 0.5 mL. If the amount of NH_4OH continued to increase, namely more than 0.5 mL, the PL intensity would decrease. It was known that NH_4OH catalyst accelerated the hydrolysis of TEOS proportionally. Rapid hydrolysis was preferred, to increase the monodispersity of the resulting particles and prevent competing reactions. Because the pH value of the solution increased with increasing NH_4OH concentration, the electrostatic stabilization of the colloid should increase. Accordingly, the ionic strength of the solution increased, which destabilized the microemulsion system.

Magnetization

Figure 7 showed the plots of the magnetization M versus the applied magnetic field H for Fe_3O_4, Fe_3O_4/SiO_2, and MPQDs at room temperature (300 K). The magnetization under applied magnetic field for all of the samples exhibited clear hysteretic behavior. It was found that both M_S

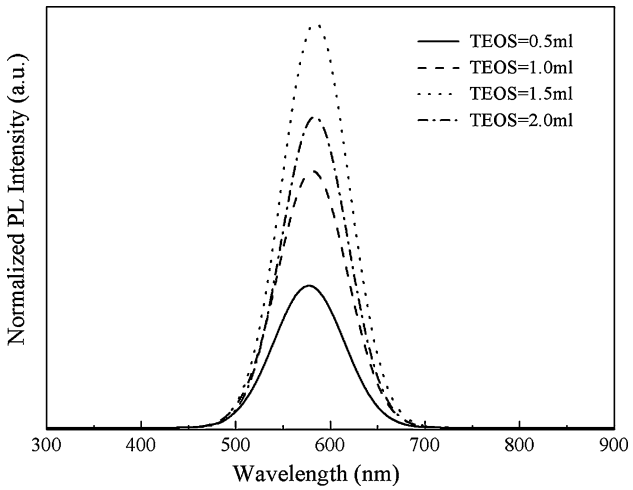

Fig. 5 The effects of the amount of TEOS on the photoluminescence spectra of the MPQDs

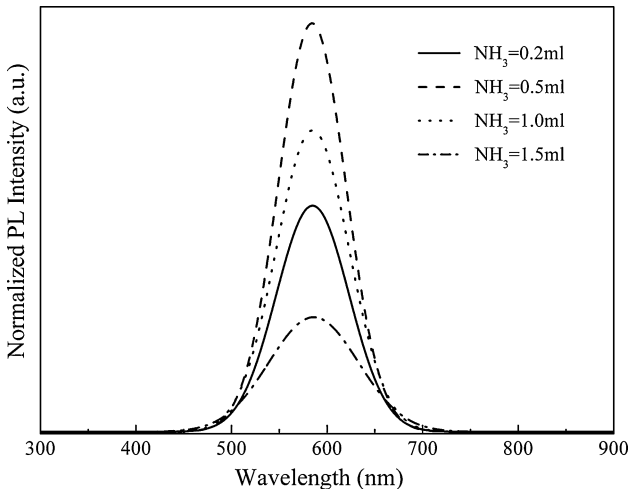

Fig. 6 The effects of the amount of ammonia on the photoluminescence spectra of the MPQDs

and H_C of Fe_3O_4/SiO_2 nanoparticles were lower than that of Fe_3O_4 nanoparticles. There have been several reports on the decrease in M_S and H_C for the magnetic nanoparticles coated with nonmagnetic matrix, when interparticle interactions have decreased via dilution [33, 34]. In addition, it was found that M_S of MPQDs (4.35 emu/g) was lower than that of Fe_3O_4/SiO_2 nanoparticles (27.59 emu/g) and Fe_3O_4 nanoparticles (65.02 emu/g). The reasons for low magnetic of MPQDs could be explained as follows: (1) On the one hand, according to the equation $M_S = \phi m_S$, M_S was related to the volume fraction of the particles (ϕ) and the saturation moment of a single particle (m_S) [35, 36]. It could be considered that the saturation magnetization of the MPQDs depended mainly on the volume fraction of Fe_3O_4 nanoparticles, due to the nonmagnetic Mn:ZnS/ZnS core–shell QDs contribution to the total magnetization, resulting in

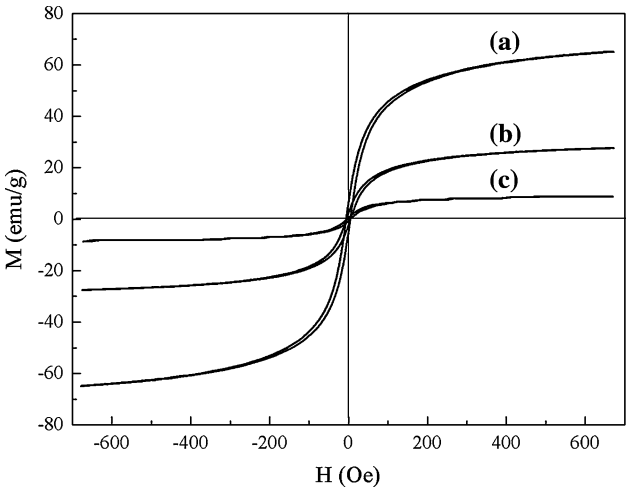

Fig. 7 Magnetic properties of Fe_3O_4 (**a**), Fe_3O_4/SiO_2 (**b**), and MPQDs (c)

the decrease in the saturation magnetization. (2) On the other hand, there may be an effect of the surface of the SiO_2 to cause a change of their magnetic property [37]. Overall, it must be concluded that the magnetic response of a system to an inert coating is rather complex and system specific, so that no firm correlations can be established at present. Therefore, the reasons for low magnetic of MPQDs should be further extensively studied in the future.

Conclusion

Water-soluble bifunctional MPQDs with Fe_3O_4 MPs and Mn:ZnS/ZnS core–shell QDs encapsulated in silica spheres were synthesized through reverse microemulsion method. The effects of the parameters for the silica coating on the surface of Fe_3O_4, such as the ratio of water to surfactant (R), the amount of NH_4OH, and the amount of TEOS, on the PL properties of MPQDs were studied. It was found that the silica coating on the surface of Fe_3O_4 could effectively suppress the interaction between the Fe_3O_4 and the QDs under the most optimal parameters, and the emission intensity of MPQDs showed a maximum. The bifunctional MPQDs prepared under the most optimal parameters have a typical diameter of 35 nm and a saturation magnetization of 4.35 emu/g at room temperature, and exhibit strong photoluminescence intensity. In a few words, the PL, magnetic, and water-soluble properties of the MPQDs would allow them to find a large range of applications for biolabeling, bioseparation, immunoassay, and diagnostics.

Acknowledgments This work was supported by the Provincial Excellent Ph.D. Thesis Research Program of Hunan (no. 2004-141) and the Graduate Educational Innovation Engineering of Central South University (no. LB08083).

References

1. M. Bruchez Jr, M. Moronne, P. Gin, S. Weiss, A.P. Alivisatos, Science **281**, 2013 (1998). doi:10.1126/science.281.5385.2013
2. W.C.W. Chan, S. Nie, Science **281**, 2016 (1998). doi:10.1126/science.281.5385.2016
3. B. Dubertret, P. Skourides, D.J. Norris, V. Noireaux, A.H. Brivanlou, A. Libchaber, Science **298**, 1759 (2002). doi:10.1126/science.1077194
4. X. Michalet, F.F. Pinaud, L.A. Bentolila, J.M. Tsay, S. Doose, J.J. Li, G. Sundaresan, A.M. Wu, S.S. Gambhir, S. Weiss, Science **307**, 538 (2005). doi:10.1126/science.1104274
5. A.M. Derfus, W.C.W. Chan, S.N. Bhatia, Nano. Lett. **4**, 11 (2004). doi:10.1021/nl0347334
6. N. Pradhan, D. Goorskey, J. Thessing, X. Peng, J. Am. Chem. Soc. **127**, 17586 (2005). doi:10.1021/ja055557z
7. N. Pradhan, D. Battaglia, Y. Liu, X. Peng, Nano. Lett. **7**, 312 (2007). doi:10.1021/nl062336y
8. N. Pradhan, X. Peng, J. Am. Chem. Soc. **129**, 3339 (2007). doi:10.1021/ja068360v
9. M. Achermann, M.A. Petruska, S.A. Crooker, V.I. Klimov, J. Phys. Chem. B **107**, 13782 (2003). doi:10.1021/jp036497r
10. J.J. Li, Y.A. Wang, W. Guo, J.C. Keay, T.D. Mishima, M.B. Johnson, X. Peng, J. Am. Chem. Soc. **125**, 12567 (2003). doi:10.1021/ja0363563
11. R.N. Bhargava, J. Lumin. **70**, 85 (1996). doi:10.1016/0022-2313(96)00046-4
12. F. Parsapour, D.F. Kelley, S. Craft, J.P. Wilcoxon, J. Chem. Phys. **104**, 4978 (1996). doi:10.1063/1.471128
13. K.E. Waldrip, J.S. Lewis III, Q. Zhai, M.R. Davidson, P.H. Holloway, S.S. Sun, Appl. Phys. Lett. **76**, 1276 (2000). doi:10.1063/1.126007
14. J.Q. Zhuang, X.D. Zhang, G. Wang, J. Mater. Chem. **13**, 1853 (2003). doi:10.1039/b303287f
15. Y. Lu, Y. Yin, B.T. Mayers, Y. Xia, Nano. Lett. **2**, 183 (2002). doi:10.1021/nl015681q
16. H. Yang, S. Zhang, X. Chen, Z. Zhuang, J. Xu, X. Wang, Anal. Chem. **76**, 1316 (2004). doi:10.1021/ac034920m
17. D. Wang, J. He, N. Rosenzweig, Z. Rosenzweig, Nano. Lett. **4**, 409 (2004). doi:10.1021/nl035010n
18. S. Santra, H. Yang, P.H. Holloway, J.T. Stanley, R.A. Mericle, J. Am. Chem. Soc. **127**, 4990 (2005). doi:10.1021/ja0428863
19. J. Kim, J.E. Lee, J. Lee, J.H. Yu, B.C. Kim, K. An, Y. Hwang, C.H. Shin, J.G. Park et al., J. Am. Chem. Soc. **128**, 688 (2006). doi:10.1021/ja0565875
20. T.R. Sathe, A. Agrawal, S. Nie, Anal. Chem. **78**, 5627 (2006). doi:10.1021/ac0610309
21. V. Salgueiriño-Maceira, M.A. Correa-Duarte, Adv. Mater. **19**, 4131 (2007). doi:10.1002/adma.200700418
22. S.T. Selvan, P.K. Patra, C.Y. Ang, J.Y. Ying, Angew. Chem. Int. Ed. **46**, 2448 (2007). doi:10.1002/anie.200604245
23. S.A. Corr, Y.P. Rakovich, Y.K. Gun'ko, Nanoscale Res. Lett. **3**, 87 (2008). doi:10.1007/s11671-008-9122-8
24. J.H. Park, G. von Maltzahn, E. Ruoslahti, S.N. Bhatia, M.J. Sailor, Angew. Chem. Int. Ed. **47**, 7284 (2008). doi:10.1002/anie.200801810
25. J.H. Gao, W. Zhang, P.B. Huang, B. Zhang, X.X. Zhang, B. Xu, J. Am. Chem. Soc. **130**, 3710 (2008). doi:10.1021/ja7103125
26. Q. Xiao, C. Xiao, Opt. Mater. **31**, 455 (2008). doi:10.1016/j.optmat.2008.06.010
27. V.S. Maceira, M.A. Correa-Duarte, M. Spasova, L.M. Liz-Marzán, M. Farle, Adv. Funct. Mater. **16**, 509 (2006). doi:10.1002/adfm.200500565
28. K.S. Suslick, G. Price, Annu. Rev. Mater. Sci. **29**, 295 (1999). doi:10.1146/annurev.matsci.29.1.295
29. H.P. Klong, *Alexander LF X-Ray Diffraction Procedures for Crystalline and Amorphous Materials* (Wiley, New York, 1954)
30. V.F. Agekyan, Phys. Solid State **44**, 2013 (2002). doi:10.1134/1.1521450
31. X. Hong, J. Li, M.J. Wang, J.J. Xu, W. Guo, J.H. Li, Y.B. Bai, T.J. Li, Chem. Mater. **16**, 4022 (2004). doi:10.1021/cm049422o
32. M. Stjerndahl, M. Andersson, H.E. Hall, D.M. Pajerowski, M.W. Meisel, R.S. Duran, Langmiur **24**, 3532 (2008). doi:10.1021/la7035604
33. X.M. Liu, S.Y. Fu, C.J. Huang, J. Magn. Magn. Mater. **281**, 234 (2004). doi:10.1016/j.jmmm.2004.04.123
34. W. Luo, S.R. Nagel, T.F. Rosenbaum, R.E. Rosensweig, Phys. Rev. Lett. **67**, 2721 (1991). doi:10.1103/PhysRevLett.67.2721
35. F. Sauzedde, A. Elaissari, C. Pichot, Colloid Polym. Sci. **277**, 846 (1999). doi:10.1007/s003960050461
36. J.C. Bacri, R. Perzynski, D. Salin, V. Cabuil, R. Massart, J. Magn. Magn. Mater. **62**, 36 (1986). doi:10.1016/0304-8853(86)90731-6
37. A.H. Lu, E.L. Salabas, F. Schüth, Angew. Chem. Int. Ed. **46**, 1222 (2007). doi:10.1002/anie.200602866